ACS Energy LETTERS

http://pubs.acs.org/journal/aelccp

A Broad-Spectrum Solid Additive to Further Boost High-Efficiency Organic Solar Cells via Morphology Regulation

Xiangjian Cao,[⊥] Jiaxin Guo,[⊥] Zhixiang Li, Xingqi Bi, Huazhe Liang, Zheng Xiao, Yaxiao Guo, Xinyuan Jia, Zheng Xu, Kangqiao Ma, Zhaoyang Yao,* Bin Kan, Xiangjian Wan, Chenxi Li, and Yongsheng Chen*

Cite This: *ACS Energy Lett.* 2023, 8, 3494−3503

Read Online

ACCESS | Metrics & More | Article Recommendations | Supporting Information

ABSTRACT: Given the great potential for achieving record breaking organic solar cells (OSCs), newly explored solid additives that could optimize nanoscale morphology of active layers have rapidly gained widespread attention. Herein, a new volatile solid additive 2,5-dichlorothieno[3,2-*b*]thiophene (TT-Cl) is delicately explored, fully satisfying the design criteria of a planar conjugated skeleton with suitable molecular size, symmetrical geometry, and proper halogenation. When applied in the state-of-the-art OSCs with diverse active layers, the quite high crystallinity of TT-Cl and strong interactions with light-harvesting components lead to optimized molecular crystalline ordering, fibrillar networks, and vertical phase distributions, thus offering a significant performance enhancement. Consequently, PM6:Y6-based binary and ternary OSCs achieved PCEs of 18.20% and 18.95%, respectively. Moreover, PM6:CH23-based binary OSCs presented an outstanding PCE of 18.72%. Our work not only provides a broad-spectrum solid additive to optimize film morphologies powerfully but also manifests great potential for achieving a record-breaking PCE of OSCs.

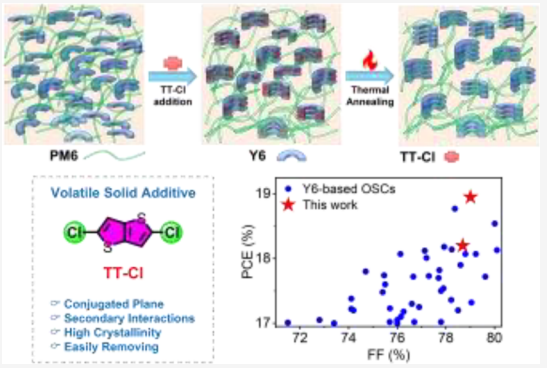

Organic solar cells (OSCs) are a promising pathway to realize efficient utilization of solar energy, and they have gained widespread traction due to their unique advantages of flexibility, large-area printability, cost-effectiveness and semitransparency.[1−10] Thus far, the state-of-the-art single-junction solar cell has reached a power conversion efficiency (PCE) of over 19%.[11,12] In such a high-performance OSC device, favorable nanoscale morphology of active layers, such as donor/acceptor (D/A) interpenetrating fibrillar network, is highly desired in light of its critically important effects on exciton diffusion and dissociation, charge transport and extraction.[13−16] However, fine regulation of film morphology in OSCs is still confronting huge challenges due to the great system complexity caused by multifactor interactions.[17−21] In general, modifying conjugated backbones or side-chains of light-harvesting materials could successfully tune molecular crystallinity, packing modes, and domain size in blended films.[22−25] Nevertheless, chemical structural changes will inevitably bring about tedious synthesis; meanwhile, there is still a lack of clear structure−morphology relationships.[26−29] As a result, several more convenient methods, including post-treatment,[25,30−34] processing additives, etc.,[35−37] have been developed with the aim of consistently establishing desired morphologies. Among them, introducing additives has been proven as a quite effective strategy to optimize molecular crystalline ordering, film fibrillar networks and even vertical distributions of light-harvesting components in OSCs.[38−40] However, the additive residues with high boiling points will result in continuous evolution of film morphology, leading to unsatisfactory long-term stability and thus rendering the additive strategy possibly infeasible for mass production of OSCs.[41,42]

Recently, as an alternative to solvent additives with high boiling points, like 1,8-diiodooctane (DIO),[43,44] volatile solid additives have been developed and demonstrated great potentials for synergistically improving PCE, stability, and

Received: June 13, 2023
Accepted: July 19, 2023
Published: July 24, 2023

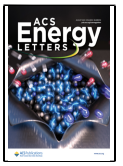

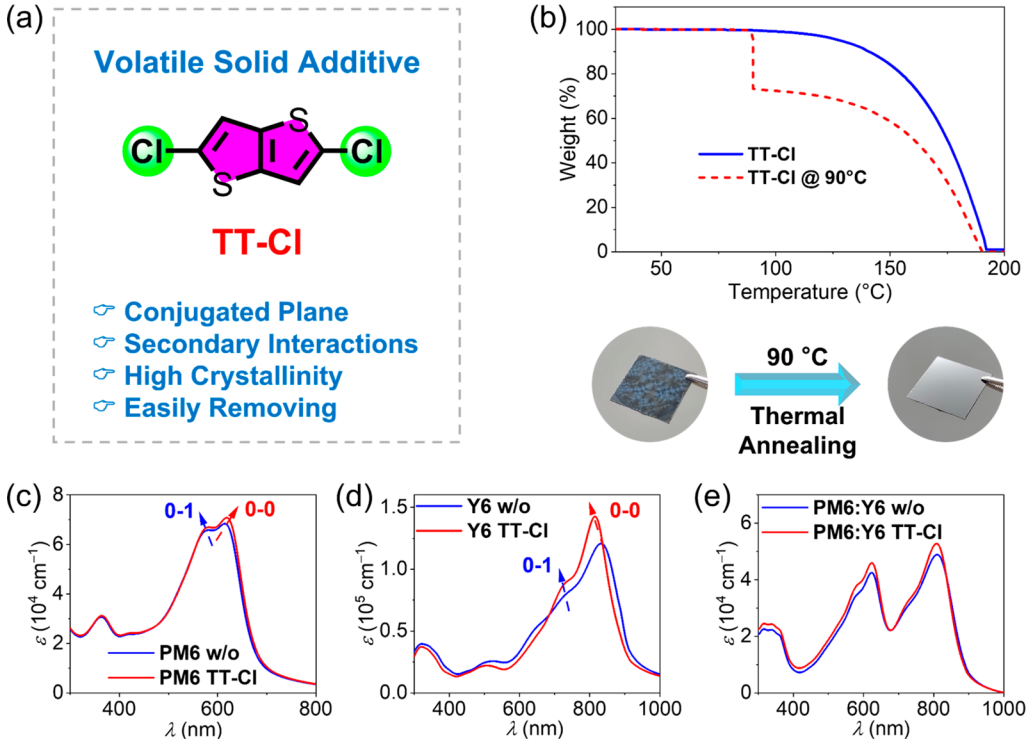

Figure 1. (a) Newly explored volatile solid additive of TT-Cl in this work. (b) Thermogravimetric analysis (TGA) curves of TT-Cl at a scan rate of 10 °C min^{-1} under a nitrogen atmosphere. The dashed curve was obtained by maintaining the sample at 90 °C for 1 h. A small amount of spin-coated TT-Cl thin film on silicon wafer can be rapidly removed after thermal annealing. UV−vis spectra of PM6 films (c), Y6 films (d), and PM6:Y6 blended films (e) with or without TT-Cl after thermal annealing at 90 °C for 5 min.

even reproducibility of OSCs.[45−47] In order to maximize the strengths of tailoring the nanoscale morphology of active layers, volatile solid additives should meet several essential criteria: (1) strong interactions with light-harvesting molecules through both $\pi-\pi$ stackings and noncovalent bonding like halogen bond, sulfur−fluorine secondary action, etc.; (2) intrinsic high crystallinity as likely a crystal seed to improve crystalline ordering of active molecules;[48] (3) ease of removal during the subsequent thermal annealing process to maintain a favorable morphology.[49] The requirements above determine that volatile solid additives are usually featured with a small but proper conjugated skeleton and preferably suitable halogenation or "soft" Lewis base atoms (like sulfur etc.) in view of chemical structures[50−52] (Figure S1). As regards to the conjugated skeletons, the simple thiophene unit would be the most likely choice as it (1) exists in all high performance OSC molecules,[53] (2) could interact with those OSC molecules through both strong $\pi-\pi$ stackings[54] and widely observed sulfur-halogen secondary interactions,[55,56] and (3) would further increase the capacity for better crystallization due to easy addition of halogen atoms on such a thiophene ring,[57] which may act as a crystal seed to optimize morphologies of active layers. In short, these combined features of simple halogenated thiophene thus would make it a promising solid additive, despite that such an analysis was rarely reported.[58]

Bearing these thoughts in mind, a new and simple solid additive, 2,5-dichlorothieno[3,2-*b*]thiophene (TT-Cl), was explored successfully (Figure 1a). The synthesis routes of TT-X (X= F, Cl, Br) and 2,6-dichlorodithieno[3,2-b:2′,3′-d]thiophene (DTT-Cl) are shown in Supporting Information (Figures S2−S5). Note that the careful selection of thieno[3,2-*b*]thiophene rather than its derived skeletons, like thiophene or dithieno[3,2-b:2′,3′-d]thiophene, is involved with multiple considerations (Figure S6): (1) the relatively smaller conjugated backbone of thiophene may not be able to offer strong enough ability of $\pi-\pi$ stacking with polymeric donors or nonfullerene acceptors; (2) although dithieno[3,2-b:2′,3′-d]thiophene affords a broad conjugated plane, its further halogenated DTT-Cl will result in a much higher temperature required for removal (Figure S7); (3) as regards to thieno[3,2-*b*]thiophene, its fluoride is faced with relatively complicated synthesis, whereas its bromide and iodide suffer from inferior chemical stability[59] and unbearably high removal temperature (Figure S8).[60] As a result, enhanced molecular crystalline ordering, superior fibrillar networks, and preferable vertical distributions of light-harvesting components can be well established when applying TT-Cl as an additive in several typical state-of-the-art OSCs, including Y6, CH, and ITIC series-based systems. Note that all of them afford clear performance enhancements, demonstrating the broad-spectrum application of TT-Cl to improve the PCE of OSCs. Among them, PCEs of 18.20% for binary-OSCs and 18.95% for ternary-OSCs based on typical and widely investigated PM6:Y6 systems have been achieved, respectively, both of which are ranked among the best values for this typical system thus far. More impressively, PM6:CH23-based binary OSCs also demonstrate an exciting PCE of 18.72% and an outstanding fill factor (FF) of 79.68% after treatment with TT-Cl, further manifesting the great potential of TT-Cl for achieving record-breaking OSCs.

As expected, such a planar and symmetrical structure of TT-Cl shows a relatively high crystallinity, which can be derived from its differential scanning calorimetry (DSC) curve (Figure

https://doi.org/10.1021/acsenergylett.3c01178
ACS Energy Lett. 2023, 8, 3494−3503

S8). Meanwhile, TT-Cl can be easily removed at a widely employed thermal annealing temperature of 90 °C during fabrication of OSCs (Figure 1b, Figure S9 and Table S1), in favor of its application as a volatile solid additive. In order to evaluate the most concerned ability of morphology regulation for TT-Cl, UV−vis spectra of PM6 and Y6 (see Figure S10 for their chemical structures) films with or without TT-Cl treatment were studied first. As shown in Figure 1c, the vibronic band between 500 and 700 nm can be assigned to internal charge transfer of PM6.[61,62] Note that an enhanced relative intensity (I_{0-0}) of 0−0 absorption can be observed with a larger intensity ratio (I_{0-0}/I_{0-1}) of 1.06 for TT-Cl treated films comparing to that of 1.04 for neat films of PM6, implying more ordered interchain stacking of PM6 after TT-Cl treating.[61,63,64] The similar tendency can be even amplified for Y6 films, indicated by the significantly enlarged I_{0-0}/I_{0-1} value of 1.62 after TT-Cl treatment (1.50 for Y6 films without TT-Cl), suggesting the greater ability of TT-Cl to tune molecular packing or micromorphology of Y6 than that of PM6 (Figure 1d). The resulting more ordered molecular packings will result in facilitated charge transport in theory, which has been proven by the both enlarged hole mobility of PM6 (1.94×10^{-4} cm^2 V^{-1} s^{-1} without TT-Cl and 3.54×10^{-4} cm^2 V^{-1} s^{-1} with TT-Cl) and electron mobility of Y6 (2.85×10^{-4} cm^2 V^{-1} s^{-1} without TT-Cl and 4.65×10^{-4} cm^2 V^{-1} s^{-1} with TT-Cl) as shown in Figure S11. Generally, when taking the enhanced absorption of PM6:Y6 blended film (Figure 1e) and enlarged charge mobility into consideration, both enlarged short circuit current density (J_{SC}) and fill factor (FF) are expected for OSCs with TT-Cl as a solid additive.

To further shed light on the influence of additives on photovoltaic behaviors, OSCs with a conventional architecture were prepared (Figure S12; see Table S2−S9 for the detailed device optimization data). The best PCE of 18.20% was yielded by OSCs based on PM6:Y6 active layer with TT-Cl, accompanied by an open circuit voltage (V_{OC}) of 0.861 V, J_{SC} of 26.86 mA cm^{-2} and FF of 78.69% (Figure 2a, and Table 1). Note that the greatly improved FF and J_{SC} compared to those of OSCs without TT-Cl agree well with our UV−vis spectra discussions above. However, the best PCE of 17.12% and 17.16% can be yielded by OSCs based on PM6:Y6 active layer treating with DTT-Cl and TT additives (Tables S3 and S6). More excitingly, a much better PCE of 18.95% along with an exciting FF of 79.01% (Figure 2b and Table 1) was further realized by a ternary OSC employing an absorption complementary donor (D18, Figure S10 and S13) as the third component. It is worth noting that this is the best PCE for Y6-based OSCs reported thus far (Figure 2c and Tables S14−S15), demonstrating the great possibility of reaching record-breaking OSCs by employing TT-Cl as solid additives. Moreover, the champion PCE of 18.35% is obtained by D18:Y6-based OSCs including a V_{OC} of 0.880 V, J_{SC} of 26.30 mA cm^{-2}, and FF of 79.27% (Table S7). Figure 2d illustrates the statistical distribution of PCEs based on 15 independent devices (see Table S10−S13 for details), revealing the evidently larger PCEs for OSCs with TT-Cl. The approximate 10% enlargement of PCEs for TT-Cl aided OSCs should mainly benefit from their greatly improved FF and J_{SC}. The enlarged external quantum efficiencies (EQEs) for OSCs with TT-Cl treating, especially in the low energy region, could result in ∼0.6 or 1.0 mA cm^{-2} amplification of integrated J_{SC} (Figure 2e,f), which is consistent with the J_{SC} values derived from $J-V$ curves. The improved EQEs of OSCs with TT-Cl should be

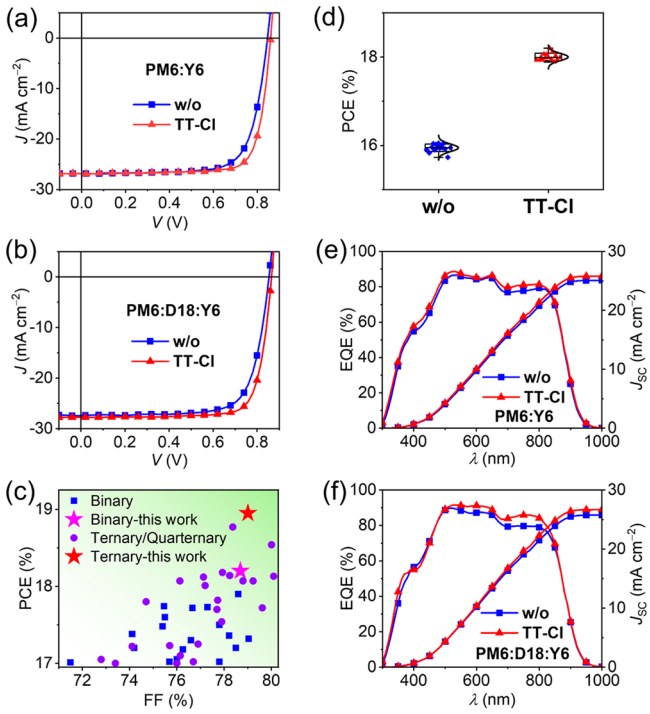

Figure 2. (a,b) $J-V$ curves of OSCs based on PM6:Y6 and PM6:D18:Y6 blends, respectively. (c) A summary of FF and PCE of OSCs based on the widely reported Y6 system (detailed parameters are listed in Tables S14−15). (d) The performance statistics of OSCs based on the typical PM6:Y6 blends. (e,f) EQE plots of OSCs based on PM6:Y6 and PM6:D18:Y6 blends, respectively.

attributed to not only the enhanced light-harvesting but also facilitated exciton/carrier dynamics. Regarding the significantly enlarged FFs, the more ordered molecular packing induced increase in charge mobilities and low energy disorder of blended films after TT-Cl treating should be taken into consideration. All the analysis above will be discussed in detail below.

Last but not least, the general applicability of TT-Cl is crucially important to its widely application in OSCs. With the exciting results for PM6:Y6-based OSCs, some other different but classic types of nonfullerene acceptors (NFAs), such as IT-4F,[65] F-2F,[66] L8-BO,[19] CH-6F,[67] and CH23[68] were further employed to blend with PM6 donor to verify the feasibility of TT-Cl. The chemical structures, $J-V$ curves, and photovoltaic parameters with and without TT-Cl have been summarized and presented in Figures S14−17 and Table 2. Similar to PM6:Y6 based devices, OSCs with these different D/A materials as active layers also manifest simultaneously improved J_{SC} and FF after TT-Cl treating. Especially, the molar absorption coefficient is enhanced in the L8-BO and CH23 neat and blended films (Figure S15). It is worth noting that PM6:CH23-based binary OSCs presented an outstanding PCE of 18.72%, which should be the record value for CH-series acceptors. The excellent general applicability of TT-Cl further emphasizes its significant potential for achieving record-breaking OSCs through tailoring nanoscale morphology of active layers, if more high-efficiency OSC systems are developed and applied in the future.

As we have mentioned above, the improved device performance with TT-Cl treating should be also determined by the superior carrier dynamics. To further unveil the origin

https://doi.org/10.1021/acsenergylett.3c01178
ACS Energy Lett. 2023, 8, 3494−3503

Table 1. Optimized Photovoltaic Parameters for OSCs[a]

Active layer	V_{OC} (V)	J_{SC} (mA cm^{-2})	Calc. J_{SC}[b] (mA cm^{-2})	FF (%)	PCE (%)
PM6:Y6 (w/o)	0.861 (0.860 ± 0.002)	26.14 (25.89 ± 0.13)	25.41	71.30 (71.58 ± 0.48)	16.05 (15.95 ± 0.09)
PM6:Y6 (TT-Cl)	0.861 (0.861 ± 0.002)	26.86 (26.71 ± 0.13)	26.15	78.69 (78.27 ± 0.30)	18.20 (18.00 ± 0.08)
PM6:D18:Y6 (w/o)	0.846 (0.845 ± 0.002)	26.84 (26.88 ± 0.19)	26.09	74.05 (73.30 ± 1.09)	16.81 (16.65 ± 0.18)
PM6:D18:Y6 (TT-Cl)	0.865 (0.859 ± 0.004)	27.73 (27.76 ± 0.12)	27.04	79.01 (78.63 ± 0.46)	18.95 (18.75 ± 0.08)

[a]Statistical results from 15 independent devices are listed in parentheses. [b]Current densities derived from EQE plots.

Table 2. Photovoltaic Parameters of Different OSCs Treated by TT-Cl[a]

Active layers	V_{OC} (V)	J_{SC} (mA cm^{-2})	Calc. J_{SC}[b] (mA cm^{-2})	FF (%)	PCE (%)
PM6:IT-4F (w/o)	0.884 (0.881 ± 0.005)	19.08 (18.94 ± 0.23)	18.60	68.16 (68.40 ± 0.16)	11.50 (11.41 ± 0.17)
PM6:IT-4F (TT-Cl)	0.869 (0.872 ± 0.003)	20.50 (20.08 ± 0.45)	20.04	75.69 (75.28 ± 0.47)	13.42 (13.16 ± 0.27)
PM6:F-2F (w/o)	0.892 (0.894 ± 0.001)	19.28 (18.89 ± 0.27)	18.77	75.45 (76.24 ± 0.80)	13.00 (12.89 ± 0.07)
PM6:F-2F (TT-Cl)	0.903 (0.902 ± 0.002)	19.34 (19.38 ± 0.05)	18.91	77.82 (77.32 ± 0.39)	13.64 (13.55 ± 0.07)
PM6:L8-BO (w/o)	0.900 (0.899 ± 0.002)	24.80 (24.59 ± 0.46)	24.07	75.38 (75.38 ± 0.34)	16.83 (16.68 ± 0.25)
PM6:L8-BO (TT-Cl)	0.906 (0.907 ± 0.002)	25.54 (25.56 ± 0.10)	24.70	79.74 (79.37 ± 0.28)	18.45 (18.39 ± 0.08)
PM6:CH-6F (w/o)	0.872 (0.872 ± 0.004)	25.55 (25.28 ± 0.19)	25.29	76.81 (76.41 ± 0.26)	17.13 (16.86 ± 0.21)
PM6:CH-6F (TT-Cl)	0.867 (0.868 ± 0.001)	26.57 (26.62 ± 0.09)	25.86	79.00 (78.61 ± 0.30)	18.21 (18.16 ± 0.04)
PM6:CH23 (w/o)	0.888 (0.887 ± 0.02)	25.43 (25.37 ± 0.12)	24.90	74.25 (74.13 ± 0.22)	16.77 (16.72 ± 0.05)
PM6:CH23 (TT-Cl)	0.879 (0.878 ± 0.001)	26.73 (26.78 ± 0.06)	25.89	79.68 (79.55 ± 0.19)	18.72 (18.62 ± 0.10)

[a]Statistical results are listed in parentheses. [b]Current densities derived from EQE plots.

of upgraded photovoltaic parameters, the exciton dissociation, charge transport, and recombination behaviors in OSCs with and without TT-Cl have been measured and analyzed by taking the typical PM6:Y6 as an example. As presented in Figure 3a, PM6:Y6-based OSC with TT-Cl treatment could yield an outstanding exciton dissociation efficiency (P_{diss}) of 98.85% and charge carrier collection efficiency (P_{coll}) of 90.55%. Note that both P_{diss} and P_{coll} are larger than those of 97.44% and 85.69% for control devices without TT-Cl, respectively. This should partially response for the enlarged EQEs[69] for OSCs with TT-Cl as discussed above. Moreover, a larger charge carrier lifetime of 0.24 ms and smaller charge extraction time of 0.37 μs can be observed from the transient photovoltage (TPV, Figure 3b) and transient photocurrent (TPC, Figure 3c) decay curves for OSCs with TT-Cl, respectively, compared to those of 0.11 ms and 0.62 μs for OSCs without TT-Cl. This indicates suppressed charge recombination and facilitated charge transport dynamics in OSCs with TT-Cl, which will also be in favor of their enlarged EQEs and FFs. Then we resorted to the space-charge limited current (SCLC) method[70−72] to further monitor the different carrier transport capacities in devices with and without TT-Cl (Figure S18 and Table S16). As displayed in Figure 3d, OSCs with TT-Cl afford both larger electron/hole mobilities of 3.47 × 10^{-4}/3.38 × 10^{-4} cm^2 V^{-1} s^{-1} than those of 2.21 × 10^{-4}/1.62 × 10^{-4} cm^2 V^{-1} s^{-1} for OSCs without TT-Cl, thus rendering a more balanced μ_e/μ_h ratio of 1.03 for OSCs with TT-Cl treatment compared to that of 1.36 for OSCs without TT-Cl. These results are also well consistent with those derived from pristine PM6 and Y6 films (Figure S11 and Figure S18). To sum up, the overall suppressed charge recombination and improved carrier mobility, in combination with a much balanced μ_e/μ_h ratio for OSCs with TT-Cl should account for the enlarged EQEs and FFs.[72]

In light of the crucial effects of favorable molecular packing on achieving superior photodynamics in OSCs, grazing incident wide-angle X-ray scattering (GIWAXS) measurements[73] were carried out to unveil the possibly diverse molecular packing behaviors with and without TT-Cl (Figure S19). Given that TT-Cl has a greater influence on small molecular NFAs such as Y6 rather than polymeric donor PM6 (Figure 1c,d), we first investigated molecular packings in Y6 pristine films. As observed in Figure 3e, both Y6-based films with or without TT-Cl show strong (010) diffraction peaks in

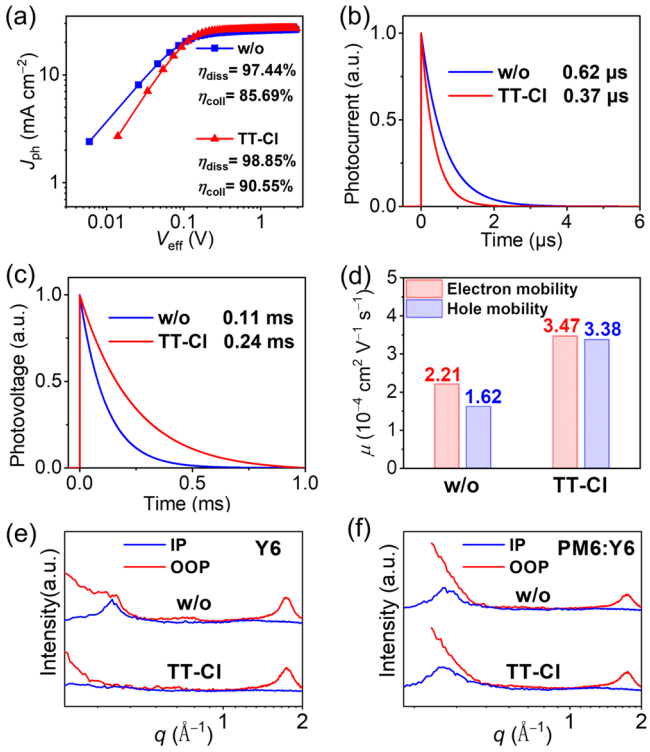

Figure 3. (a) Plots of J_{ph} versus V_{eff}. The efficiencies of charge generation and collection were also provided. (b) TPV and (c) TPC measurements of OSCs based on PM6:Y6 active layers. (d) Hole and electron mobilities of PM6:Y6-based devices with or without TT-Cl additive. (e,f) 1D line-cuts of Y6 and PM6:Y6-based films with or without TT-Cl additive, respectively, which were derived from their corresponding 2D GIWAXS patterns in Figure S19.

https://doi.org/10.1021/acsenergylett.3c01178
ACS Energy Lett. 2023, 8, 3494−3503

the out-of-plane (OOP) direction at 1.74 Å^{-1}, indicating the favorable face-on packing orientation and almost the same $\pi-\pi$ packing distance of 3.62 Å. Note that an enlarged crystal coherence length (CCL) of 29.76 Å has been afforded by Y6 with TT-Cl compared to that of 26.55 Å for Y6 without TT-Cl (Table S17), which confirms the more ordered molecular packing after TT-Cl treatment and agrees well with the enhanced 0−0 absorption discussed above (Figure 1d). Regarding PM6:Y6 or even PM6:D18:Y6 blends, an obvious enlargement of CCLs for (010) diffraction peaks in the OOP direction can be also observed after adding TT-Cl as additives, being 20.12 and 16.25 Å for PM6:Y6 with and without TT-Cl, respectively (Figure 3f and Table S18); 25.59 and 23.18 Å for PM6:D18:Y6 with and without TT-Cl, respectively (Figures S19−S20). The detailed parameters indicating the $\pi-\pi$ packing distances and CCLs are also illustrated in Table S18 for clear comparison. In theory, more ordered molecular packing suggested by both enlarged CCLs and enhanced 0−0 absorptions will result in more efficient charge transport and collection dynamics, thus in favor of improved FFs and J_{SC}s as mentioned above.[74]

It is known that D/A interpenetrating fibrillar networks are highly desirable in high-performance OSCs.[11] Therefore, atomic force microscopy (AFM) was further employed to unveil the surficial morphologies of PM6:Y6 blended films. As exhibited in Figure 4a,c, the preferable bundle-like nanofiber

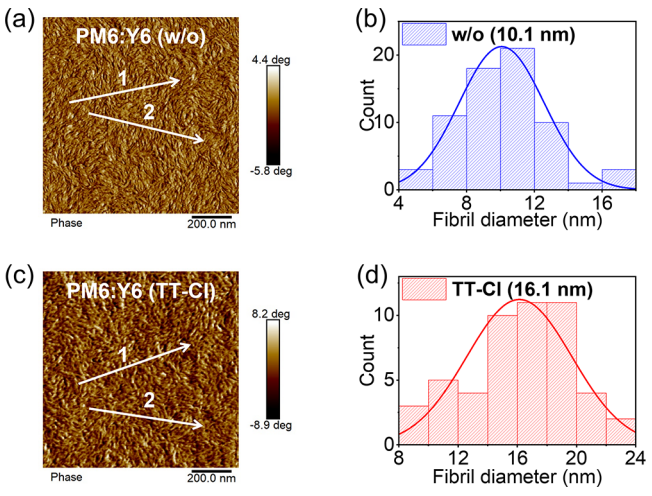

Figure 4. (a,c) AFM phase images of PM6:Y6-based films with or without TT-Cl additive, respectively. (b,d) Statistical distribution of fibril width for PM6:Y6-based films with or without TT-Cl additive (see Figure S22 for details).

network can be well constructed in both PM6:Y6 blends with and without TT-Cl. Based on a statistical size analysis (Figures S21 and S22),[75] PM6:Y6 blend with TT-Cl possesses a relatively larger average fibril diameter of 16.1 nm than both 10.1 nm without additives and 11.7 nm with TT additive (Figure 4b,d). Note that the suitable diameter (10−20 nm) of nanofibers has been verified to not only facilitate exciton dissociation and charge transport/collection dynamics but also suppress recombination of charge transfer states[76,77] and carriers effectively, thus contributing to the significantly upgraded J_{SC}s and FFs of OSCs.[78] This agrees well with our device results and photodynamic analysis for PM6:Y6-based OSCs with TT-Cl. The similar tendency of fibril diameter growing after TT-Cl treating can be also observed in PM6:D18:Y6 ternary blends, 16.5 and 15.3 nm for PM6:D18:Y6 with and without TT-Cl, respectively (Figures S23 and S24), further demonstrating the powerful capacity of tailoring nanoscale morphology of active layers using TT-Cl. The Flory−Huggins interaction parameters (χ),[79−81] which could roughly indicate the miscibility of TT-Cl with other light-harvesting components, were also estimated, being 0.90 for Y6 and 2.47 for PM6 (Figure S25 and Table S19). The significantly decreased χ for TT-Cl and Y6 suggests their much better miscibility,[82] agreeing well with the greater variation of UV−vis spectrum for Y6 with TT-Cl than that of PM6 with TT-Cl, as discussed in Figure 1c,d. Note that the quite high crystallinity of TT-Cl and relatively good miscibility with Y6 should be the response for the enlarged size of the nanofibers (Figure 4b,d).

A desirable vertical phase distribution formed in a blended film is crucially important for reaching excellent device performances. Therefore, time-of-flight secondary ion mass spectrometry (TOF-SIMS) was further performed based on PM6:Y6 blends. In view of chemical structures of PM6 and Y6, CN^- could be regarded as the indicator of Y6, whereas F^- that existing in both PM6 and Y6 can represent the total amount of light-harvesting components. In this way, the distribution of Y6 in the vertical direction can be roughly estimated through comparing the intensity ratio of CN^-/F^-. As shown in Figure 5a,b, a CN^-/F^- ratio of 1.03 was estimated in the region near hole-transport materials (PEDOT:PSS) for blended film with TT-Cl, slightly smaller than that of 1.12 for films without TT-Cl. This indicates the accumulation of PM6 near anodes after TT-Cl treating, which will facilitate charge transport and

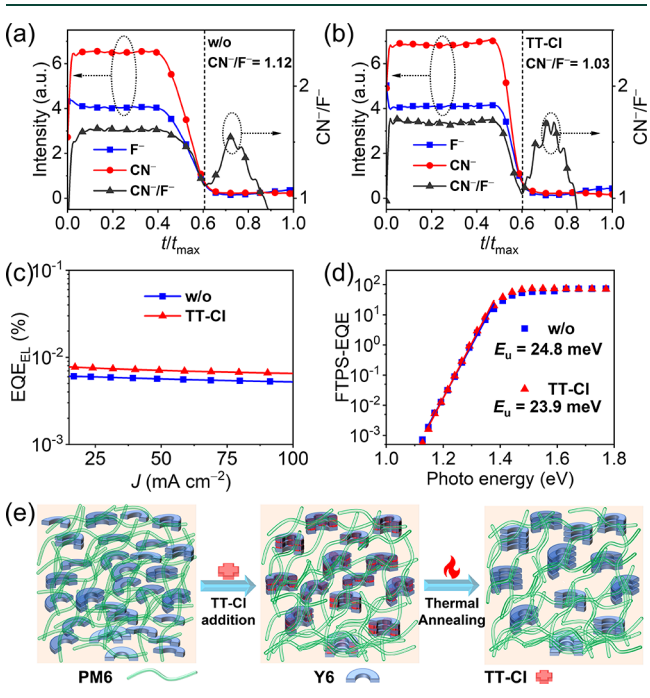

Figure 5. (a,b) Relative TOF-SIMS ion intensity of F^-, CN^- and CN^-/F^- intensity ratio as a function of t/t_{max} in PM6:Y6 BHJ films with or without TT-Cl additive. t and t_{max} are the specific and total sputtering time, respectively. (c) EQE_{EL} plots of PM6:Y6-based OSCs with or without TT-Cl additive. (d) FTPS-EQEs and fitting lines of PM6:Y6-based OSCs at absorption onset and derived Urbach energies. (e) Schematic diagram of vertical distribution of donor and acceptor in BHJ films with or without TT-Cl additive.

https://doi.org/10.1021/acsenergylett.3c01178
ACS Energy Lett. 2023, 8, 3494−3503

suppress charge recombination in theory.[83,84] Therefore, a smaller nonradiative recombination was achieved by PM6:Y6 blended film with TT-Cl treating, which can be indicated by its higher EQE_{EL} values (Figures 5c, S26 and Table S20). Furthermore, we performed Fourier transform photocurrent spectroscopy-external quantum efficiency (FTPS-EQE) to evaluate the Urbach energies quantificationally. A slightly smaller Urbach energy (E_u) of 23.9 meV for device with TT-Cl has also been afforded comparing to that of 24.8 meV for device without TT-Cl, revealing smaller energy disorders caused by more ordered molecular packing.[85,86] This is in good accordance with our discussions on UV−vis spectra and GIWAXS results above and should account for the suppressed nonradiative recombination. More importantly, the PCE of OSCs with TT-Cl could be maintained above 93% compared to their initial PCE after 480 h at 65 °C (Figure S27), which is much better than that of 79% for OSCs without TT-Cl. Moreover, Figure S28 shows the PCE variation of PM6:Y6-based OSCs by tracking at the maximum power point (MPP). OSCs without the TT-Cl additive degraded 20% of their initial PCEs within 141 h, whereas OSCs with the TT-Cl additive still maintained 85% of their initial PCE after 260 h and still demonstrated a steady-state output. The great improvement of stability should be attributed to the improved morphology and vertical phase distribution for active layers with TT-Cl treatment.

In general, after a systemic investigation involving light harvesting, photovoltaic performance, and photodynamic and morphology analysis, the carefully designed TT-Cl has been proven as a highly effective and broad-spectrum solid additive to improve the PCE and even stability of OSCs through optimizing nanoscale morphology of active layers including both preferable bundle-like nanofiber networks and vertical phase distributions (Figure 5e).

A new solid additive, 2,5-dichlorothieno[3,2-*b*]thiophene (TT-Cl), has been delicately explored to regulate the nanoscale morphology of active layers in OSCs. Benefiting from its planar conjugated skeleton with suitable molecular size, symmetrical geometry, and proper chlorination, TT-Cl could afford a quite large crystallinity as a crystal seek and possess a highly strong interaction with light-harvesting components, especially small molecular NFAs. After treating active layers with TT-Cl, significantly enhanced molecular crystalline ordering, superior fibrillar networks, and preferable vertical phase distributions could be realized, thus rendering the facilitated charge generation/transport and also suppressed nonradiative recombination. As a consequence, highly efficient and stable binary and ternary OSCs based on the typical PM6:Y6 system have been fabricated with outstanding PCEs of 18.20% and 18.95%, respectively, both of which are among the best values thus far. Moreover, TT-Cl also exhibits a broad-spectrum capacity of morphology optimization on various classic BHJ systems, further affording the best PCE value of 18.72% for CH series NFAs-based binary OSCs and verifying its great potential to be a general pathway to reach more efficient OSCs. Our success in developing the feasible solid additive not only has provided a powerful tool to tune the nanoscale morphology of active layers but also will stimulate further explorations of exotic solid additives with the aim of breaking the current PCE bottleneck of OSCs.

■ ASSOCIATED CONTENT

Supporting Information

The Supporting Information is available free of charge at https://pubs.acs.org/doi/10.1021/acsenergylett.3c01178.

Materials synthesis, device characterization and stability measurements, charge mobility, CV, UV−vis spectra and additional tables,etc. (PDF)

■ AUTHOR INFORMATION

Corresponding Authors

Yongsheng Chen − *State Key Laboratory and Institute of Elemento-Organic Chemistry, The Centre of Nanoscale Science and Technology and Key Laboratory of Functional Polymer Materials, Renewable Energy Conversion and Storage Center (RECAST), College of Chemistry, Nankai University, Tianjin 300071, China*; orcid.org/0000-0003-1448-8177; Email: yschen99@nankai.edu.cn

Zhaoyang Yao − *State Key Laboratory and Institute of Elemento-Organic Chemistry, The Centre of Nanoscale Science and Technology and Key Laboratory of Functional Polymer Materials, Renewable Energy Conversion and Storage Center (RECAST), College of Chemistry, Nankai University, Tianjin 300071, China*; orcid.org/0000-0003-1384-183X; Email: zyao@nankai.edu.cn

Authors

Xiangjian Cao − *State Key Laboratory and Institute of Elemento-Organic Chemistry, The Centre of Nanoscale Science and Technology and Key Laboratory of Functional Polymer Materials, Renewable Energy Conversion and Storage Center (RECAST), College of Chemistry, Nankai University, Tianjin 300071, China*

Jiaxin Guo − *State Key Laboratory and Institute of Elemento-Organic Chemistry, The Centre of Nanoscale Science and Technology and Key Laboratory of Functional Polymer Materials, Renewable Energy Conversion and Storage Center (RECAST), College of Chemistry, Nankai University, Tianjin 300071, China*

Zhixiang Li − *State Key Laboratory and Institute of Elemento-Organic Chemistry, The Centre of Nanoscale Science and Technology and Key Laboratory of Functional Polymer Materials, Renewable Energy Conversion and Storage Center (RECAST), College of Chemistry, Nankai University, Tianjin 300071, China*

Xingqi Bi − *State Key Laboratory and Institute of Elemento-Organic Chemistry, The Centre of Nanoscale Science and Technology and Key Laboratory of Functional Polymer Materials, Renewable Energy Conversion and Storage Center (RECAST), College of Chemistry, Nankai University, Tianjin 300071, China*

Huazhe Liang − *State Key Laboratory and Institute of Elemento-Organic Chemistry, The Centre of Nanoscale Science and Technology and Key Laboratory of Functional Polymer Materials, Renewable Energy Conversion and Storage Center (RECAST), College of Chemistry, Nankai University, Tianjin 300071, China*

Zheng Xiao − *State Key Laboratory and Institute of Elemento-Organic Chemistry, The Centre of Nanoscale Science and Technology and Key Laboratory of Functional Polymer Materials, Renewable Energy Conversion and Storage Center (RECAST), College of Chemistry, Nankai University, Tianjin 300071, China*

https://doi.org/10.1021/acsenergylett.3c01178
ACS Energy Lett. 2023, 8, 3494−3503

Yaxiao Guo − *State Key Laboratory of Separation Membranes and Membrane Processes, School of Chemistry, Tiangong University, Tianjin 300387, China*

Xinyuan Jia − *State Key Laboratory and Institute of Elemento-Organic Chemistry, The Centre of Nanoscale Science and Technology and Key Laboratory of Functional Polymer Materials, Renewable Energy Conversion and Storage Center (RECAST), College of Chemistry, Nankai University, Tianjin 300071, China*

Zheng Xu − *State Key Laboratory and Institute of Elemento-Organic Chemistry, The Centre of Nanoscale Science and Technology and Key Laboratory of Functional Polymer Materials, Renewable Energy Conversion and Storage Center (RECAST), College of Chemistry, Nankai University, Tianjin 300071, China*

Kangqiao Ma − *State Key Laboratory and Institute of Elemento-Organic Chemistry, The Centre of Nanoscale Science and Technology and Key Laboratory of Functional Polymer Materials, Renewable Energy Conversion and Storage Center (RECAST), College of Chemistry, Nankai University, Tianjin 300071, China*

Bin Kan − *School of Materials Science and Engineering, National Institute for Advanced Materials, Nankai University, Tianjin 300350, China*

Xiangjian Wan − *State Key Laboratory and Institute of Elemento-Organic Chemistry, The Centre of Nanoscale Science and Technology and Key Laboratory of Functional Polymer Materials, Renewable Energy Conversion and Storage Center (RECAST), College of Chemistry, Nankai University, Tianjin 300071, China;* orcid.org/0000-0001-5266-8510

Chenxi Li − *State Key Laboratory and Institute of Elemento-Organic Chemistry, The Centre of Nanoscale Science and Technology and Key Laboratory of Functional Polymer Materials, Renewable Energy Conversion and Storage Center (RECAST), College of Chemistry, Nankai University, Tianjin 300071, China*

Complete contact information is available at: https://pubs.acs.org/10.1021/acsenergylett.3c01178

Author Contributions

[⊥]X.C. and J.G. contributed equally. The synthetic works were carried out by J.G., X.B. and Z.X.; X.C. carried out most of the device fabrication and measurements; Z.L.; H.L. and X.J. performed the GIWAXS and E_{loss} experiments and analyzed the data; K.M. and Z.X. performed the morphology characterization and analyzed the data; Y.C. and Z.Y. supervised and directed this project; X.C.; J.G.; Z.Y., and Y.C. wrote the manuscript; All authors discussed the results and commented on the manuscript.

Notes

The authors declare no competing financial interest.

■ ACKNOWLEDGMENTS

The authors gratefully acknowledge the financial support from MoST (National Key R&D Program of China, 2022YFB4200400, 2019YFA0705900) of China and NSFC (21935007, 52025033, 51873089), Tianjin city (20JCZDJC00740, 22JCQNJC00530), 111 Project (B12015), the Fundamental Research Funds for the Central Universities, Nankai University (020-ZB22000110 and 020-92220002) and Haihe Laboratory of Sustainable Chemical Transformations.

■ REFERENCES

(1) Yang, C.; Zhang, S.; Ren, J.; Gao, M.; Bi, P.; Ye, L.; Hou, J. Molecular Design of a Non-Fullerene Acceptor Enables a P3ht-Based Organic Solar Cell with 9.46% Efficiency. *Energy Environ. Sci.* **2020**, *13* (9), 2864−2869.

(2) Zeng, G.; Chen, W.; Chen, X.; Hu, Y.; Chen, Y.; Zhang, B.; Chen, H.; Sun, W.; Shen, Y.; Li, Y.; Yan, F.; Li, Y. Realizing 17.5% Efficiency Flexible Organic Solar Cells Via Atomic-Level Chemical Welding of Silver Nanowire Electrodes. *J. Am. Chem. Soc.* **2022**, *144* (19), 8658−8668.

(3) Liu, W.; Sun, S.; Zhou, L.; Cui, Y.; Zhang, W.; Hou, J.; Liu, F.; Xu, S.; Zhu, X. Design of near-Infrared Nonfullerene Acceptor with Ultralow Nonradiative Voltage Loss for High-Performance Semi-transparent Ternary Organic Solar Cells. *Angew. Chem., Int. Ed.* **2022**, *61* (1), No. e202116111.

(4) Gillett, A. J.; Privitera, A.; Dilmurat, R.; Karki, A.; Qian, D.; Pershin, A.; Londi, G.; Myers, W. K.; Lee, J.; Yuan, J.; Ko, S.-J.; Riede, M. K.; Gao, F.; Bazan, G. C.; Rao, A.; Nguyen, T.-Q.; Beljonne, D.; Friend, R. H. The Role of Charge Recombination to Triplet Excitons in Organic Solar Cells. *Nature* **2021**, *597* (7878), 666−671.

(5) Song, W.; Liu, Y.; Fanady, B.; Han, Y.; Xie, L.; Chen, Z.; Yu, K.; Peng, X.; Zhang, X.; Ge, Z. Ultra-Flexible Light-Permeable Organic Solar Cells for the Herbal Photosynthetic Growth. *Nano Energy* **2021**, *86*, 106044.

(6) Sun, C.; Qin, S.; Wang, R.; Chen, S.; Pan, F.; Qiu, B.; Shang, Z.; Meng, L.; Zhang, C.; Xiao, M.; Yang, C.; Li, Y. High Efficiency Polymer Solar Cells with Efficient Hole Transfer at Zero Highest Occupied Molecular Orbital Offset between Methylated Polymer Donor and Brominated Acceptor. *J. Am. Chem. Soc.* **2020**, *142* (3), 1465−1474.

(7) Yu, G.; Gao, J.; Hummelen, J. C.; Wudl, F.; Heeger, A. J. Polymer Photovoltaic Cells: Enhanced Efficiencies Via a Network of Internal Donor-Acceptor Heterojunctions. *Science* **1995**, *270* (5243), 1789−1791.

(8) Li, Y.; Ji, C.; Qu, Y.; Huang, X.; Hou, S.; Li, C. Z.; Liao, L. S.; Guo, L. J.; Forrest, S. R. Enhanced Light Utilization in Semi-transparent Organic Photovoltaics Using an Optical Outcoupling Architecture. *Adv. Mater.* **2019**, *31* (40), No. 1903173.

(9) Meng, X.; Zhang, L.; Xie, Y.; Hu, X.; Xing, Z.; Huang, Z.; Liu, C.; Tan, L.; Zhou, W.; Sun, Y.; Ma, W.; Chen, Y. A General Approach for Lab-to-Manufacturing Translation on Flexible Organic Solar Cells. *Adv. Mater.* **2019**, *31* (41), No. 1903649.

(10) Wu, Q.; Yu, Y.; Xia, X. X.; Gao, Y. H.; Wang, T.; Sun, R.; Guo, J.; Wang, S. S.; Xie, G. H.; Lu, X. H.; Zhou, E. R.; Min, J. High-Performance Organic Photovoltaic Modules Using Eco-Friendly Solvents for Various Indoor Application Scenarios. *Joule* **2022**, *6* (9), 2138−2151.

(11) Zhu, L.; Zhang, M.; Xu, J.; Li, C.; Yan, J.; Zhou, G.; Zhong, W.; Hao, T.; Song, J.; Xue, X.; Zhou, Z.; Zeng, R.; Zhu, H.; Chen, C. C.; MacKenzie, R. C. I.; Zou, Y.; Nelson, J.; Zhang, Y.; Sun, Y.; Liu, F. Single-Junction Organic Solar Cells with over 19% Efficiency Enabled by a Refined Double-Fibril Network Morphology. *Nat. Mater.* **2022**, *21* (6), 656−663.

(12) Chen, T.; Li, S.; Li, Y.; Chen, Z.; Wu, H.; Lin, Y.; Gao, Y.; Wang, M.; Ding, G.; Min, J.; Ma, Z.; Zhu, H.; Zuo, L.; Chen, H. Compromising Charge Generation and Recombination of Organic Photovoltaics with Mixed Diluent Strategy for Certified 19.4% Efficiency. *Adv. Mater.* **2023**, *35* (21), 2300400.

(13) Fei, Z.; Eisner, F. D.; Jiao, X.; Azzouzi, M.; Röhr, J. A.; Han, Y.; Shahid, M.; Chesman, A. S. R.; Easton, C. D.; McNeill, C. R.; Anthopoulos, T. D.; Nelson, J.; Heeney, M. An Alkylated Indacenodithieno[3,2-B]Thiophene-Based Nonfullerene Acceptor with High Crystallinity Exhibiting Single Junction Solar Cell Efficiencies Greater Than 13% with Low Voltage Losses. *Adv. Mater.* **2018**, *30* (8), 1705209.

(14) Huang, Y.; Kramer, E. J.; Heeger, A. J.; Bazan, G. C. Bulk Heterojunction Solar Cells: Morphology and Performance Relationships. *Chem. Rev.* **2014**, *114* (14), 7006−7043.
(15) Huang, H.; Guo, Q.; Feng, S.; Zhang, C. e.; Bi, Z.; Xue, W.; Yang, J.; Song, J.; Li, C.; Xu, X.; Tang, Z.; Ma, W.; Bo, Z. Noncovalently Fused-Ring Electron Acceptors with near-Infrared Absorption for High-Performance Organic Solar Cells. *Nat. Commun.* **2019**, *10* (1), 3038.
(16) Zhang, G.; Chen, X.-K.; Xiao, J.; Chow, P. C. Y.; Ren, M.; Kupgan, G.; Jiao, X.; Chan, C. C. S.; Du, X.; Xia, R.; Chen, Z.; Yuan, J.; Zhang, Y.; Zhang, S.; Liu, Y.; Zou, Y.; Yan, H.; Wong, K. S.; Coropceanu, V.; Li, N.; Brabec, C. J.; Bredas, J.-L.; Yip, H.-L.; Cao, Y. Delocalization of Exciton and Electron Wavefunction in Non-Fullerene Acceptor Molecules Enables Efficient Organic Solar Cells. *Nat. Commun.* **2020**, *11* (1), 3943.
(17) Song, C.; Tong, L.; Liu, F.; Ye, L.; Cheng, G. J. Addressing the Reliability and Electron Transport Kinetics in Halide Perovskite Film Via Pulsed Laser Engineering. *Adv. Funct. Mater.* **2020**, *30* (5), 1906781.
(18) Zhang, X.; Li, G.; Mukherjee, S.; Huang, W.; Zheng, D.; Feng, L.-W.; Chen, Y.; Wu, J.; Sangwan, V. K.; Hersam, M. C.; DeLongchamp, D. M.; Yu, J.; Facchetti, A.; Marks, T. J. Systematically Controlling Acceptor Fluorination Optimizes Hierarchical Morphology, Vertical Phase Separation, and Efficiency in Non-Fullerene Organic Solar Cells. *Adv. Energy. Mater.* **2022**, *12* (1), 2102172.
(19) Li, C.; Zhou, J.; Song, J.; Xu, J.; Zhang, H.; Zhang, X.; Guo, J.; Zhu, L.; Wei, D.; Han, G.; Min, J.; Zhang, Y.; Xie, Z.; Yi, Y.; Yan, H.; Gao, F.; Liu, F.; Sun, Y. Non-Fullerene Acceptors with Branched Side Chains and Improved Molecular Packing to Exceed 18% Efficiency in Organic Solar Cells. *Nat. Energy* **2021**, *6* (6), 605−613.
(20) Meng, H.; Liao, C.; Deng, M.; Xu, X.; Yu, L.; Peng, Q. 18.77% Efficiency Organic Solar Cells Promoted by Aqueous Solution Processed Cobalt(Ii) Acetate Hole Transporting Layer. *Angew. Chem., Int. Ed.* **2021**, *60* (41), 22554−22561.
(21) Zhan, L.; Li, S.; Xia, X.; Li, Y.; Lu, X.; Zuo, L.; Shi, M.; Chen, H. Layer-by-Layer Processed Ternary Organic Photovoltaics with Efficiency over 18. *Adv. Mater.* **2021**, *33* (12), No. 2007231.
(22) Zhang, L.; Zhu, X.; Deng, D.; Wang, Z.; Zhang, Z.; Li, Y.; Zhang, J.; Lv, K.; Liu, L.; Zhang, X.; Zhou, H.; Ade, H.; Wei, Z. High Miscibility Compatible with Ordered Molecular Packing Enables an Excellent Efficiency of 16.2% in All-Small-Molecule Organic Solar Cells. *Adv. Mater.* **2022**, *34* (5), No. 2106316.
(23) Meng, X.; Li, M.; Jin, K.; Zhang, L.; Sun, J.; Zhang, W.; Yi, C.; Yang, J.; Hao, F.; Wang, G. W.; Xiao, Z.; Ding, L. A 4-Arm Small Molecule Acceptor with High Photovoltaic Performance. *Angew. Chem., Int. Ed.* **2022**, *61* (38), No. e202207762.
(24) An, N.; Cai, Y.; Wu, H.; Tang, A.; Zhang, K.; Hao, X.; Ma, Z.; Guo, Q.; Ryu, H. S.; Woo, H. Y.; Sun, Y.; Zhou, E. Solution-Processed Organic Solar Cells with High Open-Circuit Voltage of 1.3 V and Low Non-Radiative Voltage Loss of 0.16 V. *Adv. Mater.* **2020**, *32* (39), No. 2002122.
(25) Beaujuge, P. M.; Fréchet, J. M. J. Molecular Design and Ordering Effects in Π-Functional Materials for Transistor and Solar Cell Applications. *J. Am. Chem. Soc.* **2011**, *133* (50), 20009−20029.
(26) Fan, B.; Gao, W.; Wu, X.; Xia, X.; Wu, Y.; Lin, F. R.; Fan, Q.; Lu, X.; Li, W. J.; Ma, W.; Jen, A. K. Y. Importance of Structural Hinderance in Performance-Stability Equilibrium of Organic Photovoltaics. *Nat. Commun.* **2022**, *13* (1), 5946.
(27) Chen, H.; Zhang, R.; Chen, X.; Zeng, G.; Kobera, L.; Abbrent, S.; Zhang, B.; Chen, W.; Xu, G.; Oh, J.; Kang, S.-H.; Chen, S.; Yang, C.; Brus, J.; Hou, J.; Gao, F.; Li, Y.; Li, Y. A Guest-Assisted Molecular-Organization Approach for > 17% Efficiency Organic Solar Cells Using Environmentally Friendly Solvents. *Nat. Energy* **2021**, *6* (11), 1045−1053.
(28) Fan, B.; Lin, F.; Oh, J.; Fu, H.; Gao, W.; Fan, Q.; Zhu, Z.; Li, W. J.; Li, N.; Ying, L.; Huang, F.; Yang, C.; Jen, A. K. Y. Enabling High Efficiency of Hydrocarbon-Solvent Processed Organic Solar Cells through Balanced Charge Generation and Non-Radiative Loss. *Adv. Energy. Mater.* **2021**, *11* (41), 2101768.
(29) Liu, B.; Sun, H.; Lee, J.-W.; Yang, J.; Wang, J.; Li, Y.; Li, B.; Xu, M.; Liao, Q.; Zhang, W.; Han, D.; Niu, L.; Meng, H.; Kim, B. J.; Guo, X. Achieving Highly Efficient All-Polymer Solar Cells by Green-Solvent-Processing under Ambient Atmosphere. *Energy Environ. Sci.* **2021**, *14* (8), 4499−4507.
(30) Park, S.; Seo, Y.-S.; Shin, W. S.; Moon, S.-J.; Hwang, J. Rapid and Checkable Electrical Post-Treatment Method for Organic Photovoltaic Devices. *Sci. Rep* **2016**, *6* (1), 22604.
(31) Li, M.; Liu, F.; Wan, X.; Ni, W.; Kan, B.; Feng, H.; Zhang, Q.; Yang, X.; Wang, Y.; Zhang, Y.; Shen, Y.; Russell, T. P.; Chen, Y. Subtle Balance between Length Scale of Phase Separation and Domain Purification in Small-Molecule Bulk-Heterojunction Blends under Solvent Vapor Treatment. *Adv. Mater.* **2015**, *27* (40), 6296−6302.
(32) Chen, H.; Hsiao, Y.-C.; Hu, B.; Dadmun, M. Tuning the Morphology and Performance of Low Bandgap Polymer:Fullerene Heterojunctions Via Solvent Annealing in Selective Solvents. *Adv. Funct. Mater.* **2014**, *24* (32), 5129−5136.
(33) Kan, B.; Zhang, Q.; Li, M.; Wan, X.; Ni, W.; Long, G.; Wang, Y.; Yang, X.; Feng, H.; Chen, Y. Solution-Processed Organic Solar Cells Based on Dialkylthiol-Substituted Benzodithiophene Unit with Efficiency near 10%. *J. Am. Chem. Soc.* **2014**, *136* (44), 15529−15532.
(34) Ge, J.; Hong, L.; Song, W.; Xie, L.; Zhang, J.; Chen, Z.; Yu, K.; Peng, R.; Zhang, X.; Ge, Z. Solvent Annealing Enables 15.39% Efficiency All-Small-Molecule Solar Cells through Improved Molecule Interconnection and Reduced Non-Radiative Loss. *Adv. Energy. Mater.* **2021**, *11* (22), 2100800.
(35) Lee, J. K.; Ma, W. L.; Brabec, C. J.; Yuen, J.; Moon, J. S.; Kim, J. Y.; Lee, K.; Bazan, G. C.; Heeger, A. J. Processing Additives for Improved Efficiency from Bulk Heterojunction Solar Cells. *J. Am. Chem. Soc.* **2008**, *130* (11), 3619−3623.
(36) Zhong, L.; Kang, S. H.; Oh, J.; Jung, S.; Cho, Y.; Park, G.; Lee, S.; Yoon, S. J.; Park, H.; Yang, C. Naphthalene as a Thermal-Annealing-Free Volatile Solid Additive in Non-Fullerene Polymer Solar Cells with Improved Performance and Reproducibility. *Adv. Funct. Mater.* **2022**, *32* (33), 2201080.
(37) Peet, J.; Soci, C.; Coffin, R. C.; Nguyen, T. Q.; Mikhailovsky, A.; Moses, D.; Bazan, G. C. Method for Increasing the Photoconductive Response in Conjugated Polymer/Fullerene Composites. *Appl. Phys. Lett.* **2006**, *89* (25), 252105.
(38) Ma, Y.-F.; Zhang, Y.; Zhang, H.-L. Solid Additives in Organic Solar Cells: Progress and Perspectives. *J. Mater. Chem. C* **2022**, *10* (7), 2364−2374.
(39) Lou, S. J.; Szarko, J. M.; Xu, T.; Yu, L.; Marks, T. J.; Chen, L. X. Effects of Additives on the Morphology of Solution Phase Aggregates Formed by Active Layer Components of High-Efficiency Organic Solar Cells. *J. Am. Chem. Soc.* **2011**, *133* (51), 20661−20663.
(40) McDowell, C.; Abdelsamie, M.; Toney, M. F.; Bazan, G. C. Solvent Additives: Key Morphology-Directing Agents for Solution-Processed Organic Solar Cells. *Adv. Mater.* **2018**, *30* (33), 1707114.
(41) Huang, S.-C.; Busireddy, M. R.; Chang, H.-F.; Pan, I. C.; Ho, C.-H.; Ko, C.-W.; Tsai, Y.-W.; Lin, J.-M.; Chen, J.-T.; Hsu, C.-S. Achieving High-Performance Organic Photovoltaics by Morphology Optimization of Active Layers Using Fluorene-Based Solid Additives. *Sol. RRL* **2022**, *6* (12), 2200805.
(42) Song, J.; Li, Y.; Cai, Y.; Zhang, R.; Wang, S.; Xin, J.; Han, L.; Wei, D.; Ma, W.; Gao, F.; Sun, Y. Solid Additive Engineering Enables High-Efficiency and Eco-Friendly All-Polymer Solar Cells. *Matter* **2022**, *5* (11), 4047−4059.
(43) Sun, Y.; Welch, G. C.; Leong, W. L.; Takacs, C. J.; Bazan, G. C.; Heeger, A. J. Solution-Processed Small-Molecule Solar Cells with 6.7% Efficiency. *Nat. Mater.* **2012**, *11* (1), 44−48.
(44) Dou, L.; Gao, J.; Richard, E.; You, J.; Chen, C.-C.; Cha, K. C.; He, Y.; Li, G.; Yang, Y. Systematic Investigation of Benzodithiophene- and Diketopyrrolopyrrole-Based Low-Bandgap Polymers Designed for Single Junction and Tandem Polymer Solar Cells. *J. Am. Chem. Soc.* **2012**, *134* (24), 10071−10079.
(45) Guo, Q.; Liu, Y.; Liu, M.; Zhang, H.; Qian, X.; Yang, J.; Wang, J.; Xue, W.; Zhao, Q.; Xu, X.; Ma, W.; Tang, Z.; Li, Y.; Bo, Z.

https://doi.org/10.1021/acsenergylett.3c01178
ACS Energy Lett. 2023, 8, 3494−3503

Enhancing the Performance of Organic Solar Cells by Prolonging the Lifetime of Photogenerated Excitons. *Adv. Mater.* **2020**, *32* (50), 2003164.
(46) Li, C.; Gu, X.; Chen, Z.; Han, X.; Yu, N.; Wei, Y.; Gao, J.; Chen, H.; Zhang, M.; Wang, A.; Zhang, J.; Wei, Z.; Peng, Q.; Tang, Z.; Hao, X.; Zhang, X.; Huang, H. Achieving Record-Efficiency Organic Solar Cells Upon Tuning the Conformation of Solid Additives. *J. Am. Chem. Soc.* **2022**, *144* (32), 14731−14739.
(47) Hu, K.; Zhu, C.; Ding, K.; Qin, S.; Lai, W.; Du, J.; Zhang, J.; Wei, Z.; Li, X.; Zhang, Z.; Meng, L.; Ade, H.; Li, Y. Solid Additive Tuning of Polymer Blend Morphology Enables Non-Halogenated-Solvent All-Polymer Solar Cells with an Efficiency of over 17%. *Energy Environ. Sci.* **2022**, *15* (10), 4157−4166.
(48) Liu, L.; Kan, Y.; Gao, K.; Wang, J.; Zhao, M.; Chen, H.; Zhao, C.; Jiu, T.; Jen, A.-K. Y.; Li, Y. Graphdiyne Derivative as Multifunctional Solid Additive in Binary Organic Solar Cells with 17.3% Efficiency and High Reproductivity. *Adv. Mater.* **2020**, *32* (11), 1907604.
(49) Bao, S.; Yang, H.; Fan, H.; Zhang, J.; Wei, Z.; Cui, C.; Li, Y. Volatilizable Solid Additive-Assisted Treatment Enables Organic Solar Cells with Efficiency over 18.8% and Fill Factor Exceeding 80. *Adv. Mater.* **2021**, *33* (48), No. 2105301.
(50) Yu, R.; Yao, H.; Hong, L.; Qin, Y.; Zhu, J.; Cui, Y.; Li, S.; Hou, J. Design and Application of Volatilizable Solid Additives in Non-Fullerene Organic Solar Cells. *Nat. Commun.* **2018**, *9* (1), 4645.
(51) Song, X.; Zhang, K.; Guo, R.; Sun, K.; Zhou, Z.; Huang, S.; Huber, L.; Reus, M.; Zhou, J.; Schwartzkopf, M.; Roth, S. V.; Liu, W.; Liu, Y.; Zhu, W.; Müller-Buschbaum, P. Process-Aid Solid Engineering Triggers Delicately Modulation of Y-Series Non-Fullerene Acceptor for Efficient Organic Solar Cells. *Adv. Mater.* **2022**, *34* (20), 2200907.
(52) Ye, L.; Cai, Y.; Li, C.; Zhu, L.; Xu, J.; Weng, K.; Zhang, K.; Huang, M.; Zeng, M.; Li, T.; Zhou, E.; Tan, S.; Hao, X.; Yi, Y.; Liu, F.; Wang, Z.; Zhan, X.; Sun, Y. Ferrocene as a Highly Volatile Solid Additive in Non-Fullerene Organic Solar Cells with Enhanced Photovoltaic Performance. *Energy Environ. Sci.* **2020**, *13* (12), 5117−5125.
(53) Yan, C.; Barlow, S.; Wang, Z.; Yan, H.; Jen, A. K. Y.; Marder, S. R.; Zhan, X. Non-Fullerene Acceptors for Organic Solar Cells. *Nat. Rev. Mater.* **2018**, *3* (3), 1−19.
(54) Li, C.; Gu, X.; Chen, Z.; Han, X.; Yu, N.; Wei, Y.; Gao, J.; Chen, H.; Zhang, M.; Wang, A.; Zhang, J.; Wei, Z.; Peng, Q.; Tang, Z.; Hao, X.; Zhang, X.; Huang, H. Achieving Record-Efficiency Organic Solar Cells Upon Tuning the Conformation of Solid Additives. *J. Am. Chem. Soc.* **2022**, *144* (32), 14731−14739.
(55) Fu, J.; Chen, S.; Yang, K.; Jung, S.; Lv, J.; Lan, L.; Chen, H.; Hu, D.; Yang, Q.; Duan, T.; Kan, Z.; Yang, C.; Sun, K.; Lu, S.; Xiao, Z.; Li, Y. A "Sigma-Hole"-Containing Volatile Solid Additive Enabling 16.5% Efficiency Organic Solar Cells. *iScience* **2020**, *23* (3), 100965.
(56) Tang, M. L.; Bao, Z. Halogenated Materials as Organic Semiconductors. *Chem. Mater.* **2011**, *23* (3), 446−455.
(57) Liao, X.; Li, Q.; Ye, J.; Li, Z.; Ren, J.; Zhang, K.; Xu, Y.; Cai, Y.-P.; Liu, S.; Huang, F. Solid-Liquid Convertible Fluorinated Terthiophene as Additives in Mediating Morphology and Performance of Organic Solar Cells. *Chem. Eng. J.* **2023**, *453*, 139489.
(58) Zhang, G.; Hu, D.; Tang, H.; Song, H.; Duan, S.; Kan, Z.; Lu, S. Volatile Additive Strategy Triggering 17.48% Efficient Post-Treatment-Free Organic Solar Cells. *Sol. RRL* **2023**, *7* (4), 2200994.
(59) Ma, C.; Wang, L. Y.; Shu, M. H.; Hou, C. C.; Wang, K. X.; Chen, J. S. Thiophene Derivatives as Electrode Materials for High-Performance Sodium-Ion Batteries. *J. Mater. Chem. A* **2021**, *9* (19), 11530−11536.
(60) Sato, M.; Kubota, Y.; Tanemura, A.; Maruyama, G.; Fujihara, T.; Nakayama, J.; Takayanagi, T.; Takahashi, K.; Unoura, K. Synthesis and Some Properties of Bis(Ruthenocenyl)Thiophene Derivatives - Possible Spin-Coupling in the Two-Electron Oxidized Species of Dinuclear Ruthenocenes Bridged by Thiophene Derivatives. *Eur. J. Inorg. Chem.* **2006**, *2006* (22), 4577−4588.
(61) Liu, D.; Mun, J.; Chen, G.; Schuster, N. J.; Wang, W.; Zheng, Y.; Nikzad, S.; Lai, J.-C.; Wu, Y.; Zhong, D.; Lin, Y.; Lei, Y.; Chen, Y.; Gam, S.; Chung, J. W.; Yun, Y.; Tok, J. B. H.; Bao, Z. A Design Strategy for Intrinsically Stretchable High-Performance Polymer Semiconductors: Incorporating Conjugated Rigid Fused-Rings with Bulky Side Groups. *J. Am. Chem. Soc.* **2021**, *143* (30), 11679−11689.
(62) Sarkar, T.; Schneider, S. A.; Ankonina, G.; Hendsbee, A. D.; Li, Y.; Toney, M. F.; Frey, G. L. Tuning Intra and Intermolecular Interactions for Balanced Hole and Electron Transport in Semiconducting Polymers. *Chem. Mater.* **2020**, *32* (17), 7338−7346.
(63) Más-Montoya, M.; Janssen, R. A. J. The Effect of H- and J-Aggregation on the Photophysical and Photovoltaic Properties of Small Thiophene-Pyridine-Dpp Molecules for Bulk-Heterojunction Solar Cells. *Adv. Funct. Mater.* **2017**, *27* (16), 1605779.
(64) Spano, F. C. The Spectral Signatures of Frenkel Polarons in H- and J-Aggregates. *Acc. Chem. Res.* **2010**, *43* (3), 429−439.
(65) Zhao, W.; Li, S.; Yao, H.; Zhang, S.; Zhang, Y.; Yang, B.; Hou, J. Molecular Optimization Enables over 13% Efficiency in Organic Solar Cells. *J. Am. Chem. Soc.* **2017**, *139* (21), 7148−7151.
(66) Ke, X.; Meng, L.; Wan, X.; Li, M.; Sun, Y.; Guo, Z.; Wu, S.; Zhang, H.; Li, C.; Chen, Y. The Rational and Effective Design of Nonfullerene Acceptors Guided by a Semi-Empirical Model for an Organic Solar Cell with an Efficiency over 15%. *J. Mater. Chem. A* **2020**, *8* (19), 9726−9732.
(67) Zou, Y.; Chen, H.; Bi, X.; Xu, X.; Wang, H.; Lin, M.; Ma, Z.; Zhang, M.; Li, C.; Wan, X.; Long, G.; Zhaoyang, Y.; Chen, Y. Peripheral Halogenation Engineering Controls Molecular Stacking to Enable Highly Efficient Organic Solar Cells. *Energy Environ. Sci.* **2022**, *15* (8), 3519−3533.
(68) Liang, H.; Chen, H.; Wang, P.; Zhu, Y.; Zhang, Y.; Feng, W.; Ma, K.; Lin, Y.; Ma, Z.; Long, G.; Li, C.; Kan, B.; Yao, Z.; Zhang, H.; Wan, X.; Chen, Y. Molecular Packing and Dielectric Property Optimization through Peripheral Halogen Swapping Enables Binary Organic Solar Cells with an Efficiency of 18.77%. *Adv. Funct. Mater.* **2023**, 2301573.
(69) Chen, H.; Zou, Y.; Liang, H.; He, T.; Xu, X.; Zhang, Y.; Ma, Z.; Wang, J.; Zhang, M.; Li, Q.; Li, C.; Long, G.; Wan, X.; Yao, Z.; Chen, Y. Lowing the Energy Loss of Organic Solar Cells by Molecular Packing Engineering Via Multiple Molecular Conjugation Extension. *Sci. China Chem.* **2022**, *65* (7), 1362−1373.
(70) Haneef, H. F.; Zeidell, A. M.; Jurchescu, O. D. Charge Carrier Traps in Organic Semiconductors: A Review on the Underlying Physics and Impact on Electronic Devices. *J. Mater. Chem. C* **2020**, *8* (3), 759−787.
(71) de Boer, R. W. I.; Gershenson, M. E.; Morpurgo, A. F.; Podzorov, V. Organic Single-Crystal Field-Effect Transistors. *PHYS STATUS SOLIDI A* **2004**, *201* (6), 1302−1331.
(72) Chen, H.; Liang, H.; Guo, Z.; Zhu, Y.; Zhang, Z.; Li, Z.; Cao, X.; Wang, H.; Feng, W.; Zou, Y.; Meng, L.; Xu, X.; Kan, B.; Li, C.; Yao, Z.; Wan, X.; Ma, Z.; Chen, Y. Central Unit Fluorination of Non-Fullerene Acceptors Enables Highly Efficient Organic Solar Cells with over 18% Efficiency. *Angew. Chem., Int. Ed.* **2022**, *61* (41), No. e202209580.
(73) Müller-Buschbaum, P. The Active Layer Morphology of Organic Solar Cells Probed with Grazing Incidence Scattering Techniques. *Adv. Mater.* **2014**, *26* (46), 7692−7709.
(74) Sun, Y.; Nian, L.; Kan, Y.; Ren, Y.; Chen, Z.; Zhu, L.; Zhang, M.; Yin, H.; Xu, H.; Li, J.; Hao, X.; Liu, F.; Gao, K.; Li, Y. Rational Control of Sequential Morphology Evolution and Vertical Distribution toward 17.18% Efficiency All-Small-Molecule Organic Solar Cells. *Joule* **2022**, *6* (12), 2835−2848.
(75) Ma, K.; Liang, H.; Wang, Y.; Xiao, Z.; Jiang, C.; Feng, W.; Zhang, Z.; Si, X.; Liu, J.; Wan, X.; Kan, B.; Li, C.; Yao, Z.; Chen, Y. New Type of Polymerized Small a-D-a Acceptors Constructed by Conjugation Extension in the Branched Direction. *ACS Mater. Lett.* **2023**, *5* (3), 884−892.
(76) Chen, X. K.; Qian, D. P.; Wang, Y. M.; Kirchartz, T.; Tress, W.; Yao, H. F.; Yuan, J.; Hulsbeck, M.; Zhang, M. J.; Zou, Y. P.; Sun, Y. M.; Li, Y. F.; Hou, J. H.; Inganas, O.; Coropceanu, V.; Bredas, J. L.;

https://doi.org/10.1021/acsenergylett.3c01178
ACS Energy Lett. 2023, 8, 3494−3503

Gao, F. A Unified Description of Non-Radiative Voltage Losses in Organic Solar Cells. *Nat. Energy* **2021**, *6* (8), 799−806.
(77) Chong, K.; Xu, X.; Meng, H.; Xue, J.; Yu, L.; Ma, W.; Peng, Q. Realizing 19.05% Efficiency Polymer Solar Cells by Progressively Improving Charge Extraction and Suppressing Charge Recombination. *Adv. Mater.* **2022**, *34* (13), No. 2109516.
(78) Kirchartz, T.; Agostinelli, T.; Campoy-Quiles, M.; Gong, W.; Nelson, J. Understanding the Thickness-Dependent Performance of Organic Bulk Heterojunction Solar Cells: The Influence of Mobility, Lifetime, and Space Charge. *J. Phys. Chem. Lett.* **2012**, *3* (23), 3470−3475.
(79) Campoy-Quiles, M.; Ferenczi, T.; Agostinelli, T.; Etchegoin, P. G.; Kim, Y.; Anthopoulos, T. D.; Stavrinou, P. N.; Bradley, D. D. C.; Nelson, J. Morphology Evolution Via Self-Organization and Lateral and Vertical Diffusion in Polymer:Fullerene Solar Cell Blends. *Nat. Mater.* **2008**, *7* (2), 158−164.
(80) Honda, S.; Ohkita, H.; Benten, H.; Ito, S. Selective Dye Loading at the Heterojunction in Polymer/Fullerene Solar Cells. *Adv. Energy. Mater.* **2011**, *1* (4), 588−598.
(81) Nilsson, S.; Bernasik, A.; Budkowski, A.; Moons, E. Morphology and Phase Segregation of Spin-Casted Films of Polyfluorene/Pcbm Blends. *Macromolecules* **2007**, *40* (23), 8291−8301.
(82) Feng, W.; Wu, S.; Chen, H.; Meng, L.; Huang, F.; Liang, H.; Zhang, J.; Wei, Z.; Wan, X.; Li, C.; Yao, Z.; Chen, Y. Tuning Morphology of Active Layer by Using a Wide Bandgap Oligomer-Like Donor Enables Organic Solar Cells with over 18% Efficiency. *Adv. Energy. Mater.* **2022**, *12* (16), 2104060.
(83) Zhan, L.; Li, S.; Xia, X.; Li, Y.; Lu, X.; Zuo, L.; Shi, M.; Chen, H. Layer-by-Layer Processed Ternary Organic Photovoltaics with Efficiency over 18%. *Adv. Mater.* **2021**, *33* (12), 2007231.
(84) Xu, X.; Jing, W.; Meng, H.; Guo, Y.; Yu, L.; Li, R.; Peng, Q. Sequential Deposition of Multicomponent Bulk Heterojunctions Increases Efficiency of Organic Solar Cells. *Adv. Mater.* **2023**, *35* (12), 2208997.
(85) Zhang, Z.; Li, Y.; Cai, G.; Zhang, Y.; Lu, X.; Lin, Y. Selenium Heterocyclic Electron Acceptor with Small Urbach Energy for as-Cast High-Performance Organic Solar Cells. *J. Am. Chem. Soc.* **2020**, *142* (44), 18741−18745.
(86) Liu, S.; Yuan, J.; Deng, W.; Luo, M.; Xie, Y.; Liang, Q.; Zou, Y.; He, Z.; Wu, H.; Cao, Y. High-Efficiency Organic Solar Cells with Low Non-Radiative Recombination Loss and Low Energetic Disorder. *Nat. Photonics* **2020**, *14* (5), 300−305.

https://doi.org/10.1021/acsenergylett.3c01178
ACS Energy Lett. 2023, 8, 3494−3503